

Mono- and Trinuclear Cu^{II} Complexes with Tripodal Ligands

Yukinari Sunatsuki,[1] Tamami Kobayashi,[1] Kenji Harada,[1] Tomoka Yamaguchi,[1] Matsuo Nonoyama,[2] and Masaaki Kojima*[1]

[1]Department of Chemistry, Faculty of Science, Okayama University, 3-1-1 Tsushima-naka, Okayama 700-8530

[2]Department of Chemistry, Faculty of Science, Nagoya University, Chikusa-ku, Nagoya 464-8602

Received October 15, 2007; E-mail: kojima@cc.okayama-u.ac.jp

Mononuclear [Cu(HL)] (**1**) and trinuclear $[Cu_3(L)_2]$ (**3**) complexes were synthesized, where H_3L (1,1,1-tris[(salicylideneamino)methyl]ethane) is a tripodal ligand obtained by condensation of 1,1,1-tris(aminomethyl)ethane and salicylaldehyde in a 1:3 mole ratio. Another mononuclear complex [Cu(HL′)] (**2**), where one of the three arms was disconnected probably due to thermal hydrolysis, was also obtained. The crystal structures, electronic spectra, and electrochemical and magnetic properties of the complexes were studied. In **1**, one of the arms of H_3L is not coordinated to the metal atom, and the ligand serves as a tetradentate N_2O_2 ligand, the complex assuming a slightly distorted square-planar structure. In the trinuclear complex, an imine nitrogen atom and a phenolate oxygen atom of one arm of each terminal unit coordinate to the central Cu^{II} ion to form a linear trinuclear complex. The coordination geometry about each Cu is square planar. All of the complexes involve π–π stacking interactions between the molecules in the crystal structures, which are responsible for weak magnetic interactions. An electrochemical study of **3** in DMSO showed that the central Cu^{II} is more easily reduced to Cu^{I} than the terminal Cu ions. The mononuclear complexes, **1** and **2**, show a quasi-reversible $Cu^{II/I}$ couple almost at the same position as that of the terminal Cu ions of **3**.

Metal complexes containing tripodal Schiff base ligands derived from 1:3 condensation of 1,1,1-tris(aminomethyl)alkane and salicylaldehyde or its derivatives have attracted much attention.[1–12] For example, we have reported that 1,1,1-tris[(salicylideneamino)methyl]ethane (H_3L, Figure 1a) forms a relatively rare octahedral silicon(IV) complex, $[Si^{IV}(L)]^+$ and that the complex is stable toward hydrolysis probably because of the half-cage structure, and we could resolve the complex into its enantiomers.[8] Recently, we prepared two types of nickel(II) complexes, $[Ni^{II}(HL)]$ and $[Ni\{Ni(L)\}_2]$.[9–11] In $[Ni\{Ni(L)\}_2]$, each terminal Ni^{II} ion is coordinated by the L^{3-} ligand in an octahedral fashion and functions as a tridentate ligand, and the central Ni^{II} ion is bridged by six phenolate oxygen atoms to the terminal Ni^{II} ions to form a linear trinuclear complex (Figure 1c). We have also prepared face-sharing trioctahedral homometal 3d complexes such as $[Co^{II}_2(L)_3]$ and $[Fe^{II}_2(L)_3]$.[12] By using $[Ni^{II}(L)]^-$ as a complex ligand, we were able to prepare 3d heterometal Ni–M–Ni-type complexes such as $[Mn^{II}\{Ni(L)\}_2]$, and $[Fe^{III}\{Ni(L)\}_2]^+$.[13] By employing the same strategy, we have prepared 3d–4f complexes such as a Ni^{II}–Gd^{III} system.[14] We isolated dinuclear $Ni^{II}Gd^{III}$, trinuclear $Ni^{II}Gd^{III}Ni^{II}$, and tetranuclear $Ni^{II}Gd^{III}Gd^{III}Ni^{II}$ complexes, where the product identity depends on the nature of the ancillary ligands used.

The copper(II) ion assumes a variety of coordination numbers, 3–8, the most common ones being 4, 5, and 6. 4-Coordinated square-planar and 6-coordinated tetragonally distorted coordination are quite common, while complexes with regular octahedral geometry are not easily made because of the Jahn–Teller effect. We have prepared two copper(II) complexes containing H_3L, the complexes being formulated as [Cu(HL)] and $[Cu_3(L)_2]$. We report here the synthesis, crystal structures, electronic spectra, and electrochemical and magnetic properties of the complexes. Although the chemical formulas of the

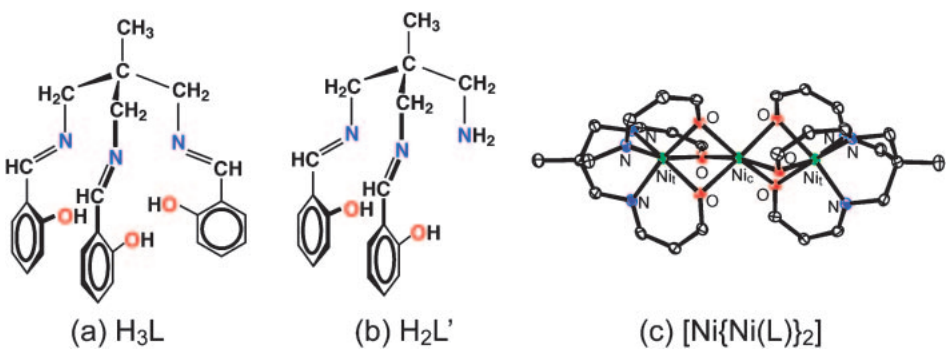

Figure 1. (a) The H_3L ligand. (b) The H_2L' ligand. (c) ORTEP view of $[Ni\{Ni(L)\}_2]$, the H atoms and aromatic moieties being omitted for clarity.

Published on the web June 11, 2008; doi:10.1246/bcsj.81.716

Cu^{II} and Ni^{II} complexes are the same, $[M^{II}(HL)]$ and $[M^{II}_3(L)_2]$ (M = Cu and Ni), the coordination arrangements around the metal ions are different; square planar (Cu) vs. octahedral (Ni). In the course of preparation of the mononuclear complex, we obtained a complex containing a partly decomposed ligand, where one of the three arms was disconnected. The structure and properties of this complex are also reported.

Results and Discussion

Synthesis and Characterization. The reaction of $Cu(CH_3COO)_2 \cdot H_2O$ with H_3L in a 1:1 mole ratio afforded a mixture of mononuclear complex, [Cu(HL)] (**1**), and the trinuclear complex, $[Cu_3(L)_2]$. The exclusive formation of the mononuclear complex was achieved by the reaction of Cu^{II} with H_3L in a 1:3 mole ratio in the absence of a base. As will be shown later, the mononuclear complex **1** has a slightly distorted square-planar structure and one of the arms is not coordinated to the metal atom. In the trinuclear complex, $[Cu_3(L)_2]$, an imine nitrogen atom and a phenolate oxygen atom of one arm of each terminal unit coordinate to the central Cu^{II} ion to form a trinuclear complex. The H_3L ligand is not so soluble in ethanol and in order to increase the reactivity we tried to dissolve it (1 molar equivalent) on heating in the presence of triethylamine (0.5 molar equivalent), and then the solution was allowed to react with $Cu(ClO_4)_2 \cdot 6H_2O$ (0.5 molar equivalent). The IR spectrum of the product **2** showed absorption bands around 1100 and 3131 cm^{-1} assignable to the Cl–O (ClO_4^-) and N–H ($-NH_3^+$) stretching band, respectively.[15] Elemental analysis and X-ray crystal structure determination (see below) of the product showed that one of the arms of the tripodal ligand was detached, probably due to thermal hydrolysis, and the resulting amino group is protonated. The structure of the partly decomposed ligand, H_2L', is shown in Figure 1b. Complex **2** is formulated as $[Cu(HL')]ClO_4$. The trinuclear complexes, $[Cu_3(L)_2] \cdot CH_3CN \cdot 2CH_3OH$ (**3**) and $[Cu_3(L)_2] \cdot 2CH_2Cl_2$ (**4**), were prepared by reaction of $Cu(CH_3COO)_2 \cdot H_2O$ with H_3L in the presence of triethylamine (3:2:6), acetonitrile–methanol, and dichloromethane being used as solvent, respectively.

Electronic Spectra. The electronic spectra of [Cu(HL)] (**1**), $[Cu(HL')]ClO_4$ (**2**), and $[Cu_3(L)_2] \cdot CH_3CN \cdot 2CH_3OH$ (**3**) in DMSO are shown in Figure 2 together with those of [Cu(salen)] (H_2salen = *N*,*N*′-disalicylideneethylenediamine) and H_3L, the data being listed in Table 1. The spectral patterns of **1**–**3** are very similar to each other, although the intensity of **3** is about three times as large as those of **1** and **2**. These results are somewhat unexpected, because the X-ray structure analyses showed differences in the coordination geometry (the degree of distortion from planarity) and arrangement (cis/trans) of the donor atoms among the complexes (see below). The electronic spectrum of $[Cu_3(L)_2] \cdot 2CH_2Cl_2$ (**4**) is identical to that of **3**. The low-intensity absorption bands at 616 nm (16250 cm^{-1}, 160 $M^{-1}\,cm^{-1}$, **1**), 612 nm (16340 cm^{-1}, 205 $M^{-1}\,cm^{-1}$, **2**), and 613 nm (16330 cm^{-1}, 582 $M^{-1}\,cm^{-1}$, **3**) are assigned to the d–d transitions.[16] The electronic spectra of square-planar copper(II) complexes containing Schiff base ligands derived from salicylaldehyde and diamine (2:1) have been reported previously.[16–18] In particular, the spectra of [Cu(salen)] and its derivatives have been investigated extensively. Although the spectral patterns of **1**–**3** are similar to that of [Cu(salen)] (Figure 2), the d–d band maxima of **1**–**3** are at lower energies than that of [Cu(salen)] (580 nm, 17260 cm^{-1}) and the shift may be attributed to the six-membered chelate ring of the N–N moiety for **1**–**3** as opposed to the five-membered ring for [Cu(salen)]. It has been reported that substitution of trimethylenediamine (tn) for ethylenediamine (en) causes a red shift of the d–d transitions; the d–d band maximum of [Cu(saltn)] (H_2saltn = *N*,*N*′-disalicylidenetrimethylenediamine) is observed at 605 nm (16500 cm^{-1}).[19]

At higher energies, **1** (369 nm, 27100 cm^{-1}, 9240 $M^{-1}\,cm^{-1}$), **2** (370 nm, 27000 cm^{-1}, 10300 $M^{-1}\,cm^{-1}$), **3** (372 nm, 26900 cm^{-1}, 31500 $M^{-1}\,cm^{-1}$), and [Cu(salen)] (363 nm, 27500 cm^{-1}, 11200 $M^{-1}\,cm^{-1}$) exhibit an intense band attributable to a π–π^* transition originating in the imine chromophore.[16] Compared with the position of the free H_3L ligand (318 nm, 31500 cm^{-1}, 13600 $M^{-1}\,cm^{-1}$), the bands for **1**, **2**, and **3** have undergone a red shift of 51, 52, and 54 nm, respectively. Such shifts are expected because coordination to a metal ion increases the extent of conjugation in the molecules.[20]

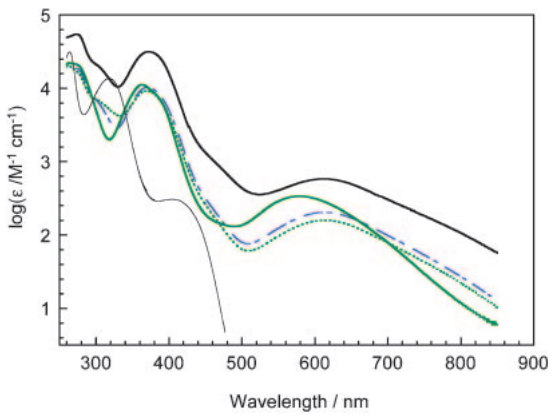

Figure 2. Electronic spectra of copper(II) complexes in DMSO; [Cu(HL)] (**1**, ····), $[Cu(HL')]ClO_4$ (**2**, —·—), $[Cu_3(L)_2] \cdot CH_3CN \cdot 2CH_3OH$ (**3**, —), [Cu(salen)] (—), and H_3L (—).

Table 1. Electronic Spectral Data of [Cu(HL)] (**1**), $[Cu(HL')]ClO_4$ (**2**), $[Cu_3(L)_2] \cdot CH_3CN \cdot 2CH_3OH$ (**3**), [Cu(salen)], and H_3L in DMSO

Compound	λ/nm (ε/$M^{-1}\,cm^{-1}$)
1	261 (20700), 280 (sh, 14300), 300 (sh, 7100), 369 (9240), 616 (160)
2	261 (19300), 280 (sh, 16200), 300 (sh, 7000), 370 (10300), 612 (205)
3	273 (54900), 300 (sh, 21300), 372 (31500), 613 (582)
[Cu(salen)]	269 (21700), 295 (sh, 7430), 363 (11200), 580 (337)
H_3L	264 (31400), 318 (13600)

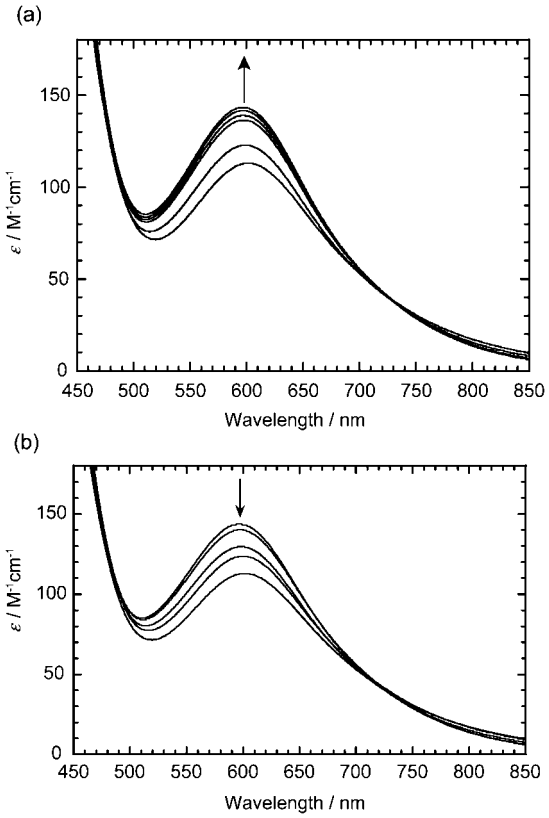

Figure 3. The pH-dependent electronic spectra of [Cu(HL)] (**1**) for the (a) forward and (b) reverse titration. A methanol solution (5 cm^3) of **1** (2.5 mM) was prepared, and the spectrum was measured after each 0.13 cm^3 addition of 0.02 M NaOMe solution, until 1 molar equivalent of the base was added. Immediately afterward, the electronic spectra were recorded for the reverse titration, 0.13 cm^3 aliquots of 0.02 M HCl solution being added. The spectra were corrected for the volume variation caused by the addition of base or acid solution.

At still higher energies, intense bands attributable to benzene π–π^* transitions are observed.[21] All these observations are in accordance with a square-planar structure of **1**–**3** with an N_2O_2 chromophore just like [Cu(salen)] (see below).

The pH-dependent electronic spectra of **1** were measured: a methanol solution (5 cm^3) of **1** (2.5 mM, 1 M = 1 mol dm^{-3}) was prepared, and the spectrum was measured after each 0.13 cm^3 addition of 0.02 M NaOMe solution, until 1 molar equivalent of the base had been added. Immediately afterward, the electronic spectra were recorded for the reverse titration, 0.13 cm^3 aliquots of 0.02 M HCl solution being added. The spectra were corrected for the volume variation caused by the addition of base or acid. The forward and reverse spectral changes are shown in Figure 3a and Figure 3b, respectively. The reverse titration converted to the spectrum of **1**, demonstrating that the reaction is reversible. The forward process is associated with the deprotonation of the uncoordinated phenol group, and the band at ca. 600 nm shifts to a shorter wavelength and increases in intensity. The spectral change may be related to the formation of a six-coordinate species, $[Cu(L)]^-$, with a distorted octahedral structure.

Electrochemistry. The electrochemical behavior of [Cu(HL)] (**1**), $[Cu(HL')]ClO_4$ (**2**), $[Cu_3(L)_2]\cdot CH_3CN\cdot 2CH_3OH$ (**3**), and [Cu(salen)] was studied in DMSO by cyclic voltammetry and coulometry, the data being listed in Table 2. The cyclic voltammogram of **3** in DMSO showed quasi-reversible couples at −1.04 and −1.34 V vs. Ag/Ag^+ (Figure 4). The wave heights suggest that the couple at −1.04 V involves one-electron transfer and that at −1.34 V two-electron transfer. Coulometry at −1.1 V indicated one-electron transfer and that at −1.4 V three-electron transfer. The green solution became brownish yellow after three-electron reduction. From these results, we conclude that the couple at −1.04 V is associated with the redox ($Cu^{II/I}$) of the central copper ion, and the couple at −1.34 V with that of the terminal copper ions; the central Cu^{II} is more easily reduced to Cu^{I} than the terminal Cu ions. [Cu(salen)] showed a quasi-reversible $Cu^{II/I}$ redox couple at −1.47 V, and the quasi-reversible redox couple of **1** (−1.27 V) is almost at the same position as that of the terminal copper ions of **3** (−1.34 V). The electrochemical behavior of **2** is quite similar to that of **1**. These results for the mononuclear complexes are in accordance with the assignments for the trinuclear complex, **3**. The fact that the central Cu^{II} ion is more easily

Table 2. Electrochemical Data[a] of [Cu(HL)] (**1**), $[Cu(HL')]ClO_4$ (**2**), $[Cu_3(L)_2]\cdot CH_3CN\cdot 2CH_3OH$ (**3**), and [Cu(salen)] (vs. Ag/Ag^+)

Complex	E_{pa}/V	E_{pc}/V	ΔE_p/mV	$E^{0'}$/V
1	−1.20	−1.34	140	−1.27
2	−1.25	−1.35	100	−1.30
3	−0.99	−1.08	90	−1.04
	−1.27	−1.40	130	−1.34
[Cu(salen)]	−1.43	−1.51	80	−1.47

a) By cyclic voltammetry in DMSO containing 0.1 M Bu_4NBF_4 at a glassy carbon electrode with a scan rate of 100 mV s^{-1}.

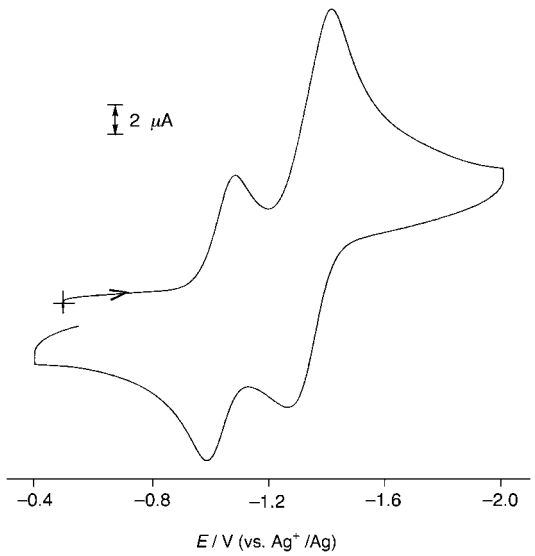

Figure 4. Cyclic voltammogram of $[Cu_3(L)_2]\cdot CH_3CN\cdot 2CH_3OH$ (**3**) in DMSO containing 0.1 M Bu_4NBF_4; scan rate, 100 mV s^{-1}; working electrode, glassy carbon; auxiliary electrode, platinum wire; reference electrode, Ag/Ag^+.

Table 3. X-ray Crystallographic Data for [Cu(HL)] (**1**), [Cu(HL′)]ClO_4 (**2**), $[Cu_3(L)_2]\cdot CH_3CN\cdot 2CH_3OH$ (**3**), and $[Cu_3(L)_2]\cdot 2CH_2Cl_2$ (**4**)

	1	**2**	**3**	**4**
Formula	$C_{26}H_{25}CuN_3O_3$	$C_{19}H_{22}ClCuN_3O_6$	$C_{56}H_{59}Cu_3N_7O_8$	$C_{54}H_{52}Cu_3Cl_4N_6O_6$
Formula weight	491.04	487.4	1148.75	1209.46
Crystal system	triclinic	monoclinic	triclinic	triclinic
Space group	$P\bar{1}$ (No. 2)	$P2_1/c$ (No. 14)	$P\bar{1}$ (No. 2)	$P\bar{1}$ (No. 2)
a/Å	11.2711(3)	10.641(3)	11.5062(4)	9.6066(3)
b/Å	13.0802(3)	11.106(3)	13.0414(4)	12.0468(3)
c/Å	17.4670(5)	17.996(6)	17.7948(7)	12.2624(4)
α/°	108.3265(9)	90	93.2223(12)	105.6230(10)
β/°	90.3078(9)	98.034(12)	106.8339(12)	107.1180(10)
γ/°	115.4161(7)	90	90.6304(11)	97.6770(9)
V/Å^3	2178.16(10)	2105.8(10)	2550.73(15)	1270.73(7)
Z	4	4	2	1
D_{calcd}/g cm^{-3}	1.497	1.537	1.493	1.580
μ/cm^{-1}	10.378	12.049	13.03	15.119
R_1[a] [$I > 2.0\sigma(I)$]	0.0478	0.0369	0.0807	0.0582
wR_2[b] [all data]	0.1341	0.0967	0.2244	0.1696
T/°C	−180	−180	−180	−180

a) $R_1 = \Sigma||F_o| - |F_c||/\Sigma|F_o|$. b) $wR_2 = [\Sigma(w(F_o^2 - F_c^2)^2/\Sigma wF_o^2)^2]^{1/2}$.

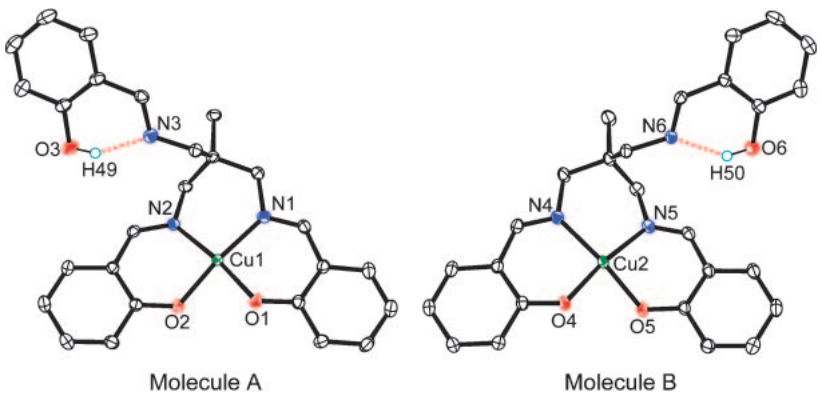

Figure 5. ORTEP views of the two independent molecules **A** and **B** of [Cu(HL)] (**1**) with atom numbering scheme showing the 50% probability ellipsoids. Hydrogen atoms, except for those attached to phenolic oxygen atoms, O3 and O6, are omitted for clarity. Color code: green, Cu; blue, N; red, O; black, C.

reduced to Cu^I than the terminal copper ions and those of **1** and **2** may be related to the *trans*-N_2O_2 structure (see below).

Structural Description of [Cu(HL)] (1). Compound **1** crystallized in the triclinic space group $P\bar{1}$ (No. 2) with $Z = 4$. The crystal data are summarized in Table 3. Compound **1** contains two independent molecules, **A** (Cu(1)) and **B** (Cu(2)), in the crystal. Figure 5 shows perspective views of these two molecules with atom numbering schemes. Selected bond distances and angles are listed in Table 4. The molecular structures of **A** and **B** are similar to each other. Although the H_3L ligand is potentially hexadentate, one of the arms is not coordinated to the metal atom, and the ligand serves as a tetradentate N_2O_2 ligand in **1**. The uncoordinated phenolic oxygen atoms, O(3) and O(6), are not deprotonated and the ligand in the complex can be expressed as HL^{2-}. The phenolic hydrogen atoms, H(49) and H(50), are hydrogen bonded to the imine nitrogen atoms, N(3) and N(6), with distances of O(3)···N(3) = 2.602(3) Å and O(6)···N(6) = 2.610(2) Å. The coordination geometry around each copper is slightly distorted square planar. The dihedral angle between the Cu(1)–N(1)–O(1) and Cu(1)–N(2)–O(2) planes is 2.60°, and that between the Cu(2)–N(4)–O(4) and Cu(2)–N(5)–O(5) planes is 5.17°. As Figure 6a shows, **A** and **B** are π–π stacked with **A′** (Cu(1′)) and **B′** (Cu(2′)), respectively, to form dimeric structures, where **A′** and **B′** are related to **A** and **B** by an inversion operation, the inversion centers being at the midpoints of the Cu(1)···Cu(1′) and Cu(2)···Cu(2′). The Cu(1)···Cu(1′) and Cu(2)···Cu(2′) distances are 3.3116(4) and 3.1084(5) Å, respectively, suggesting that direct interaction between the metal ions will be very small. Stacking is observed between ligand moieties including O(phenolate)–C(aromatic)–C(aromatic)–C(imine)–N(imine). The average stacking distance is 3.33 Å for **A**–**A′** and 3.18 Å for **B**–**B′**. Because the two mononuclear units of a dimer are related by an inversion center, the two mean coordination planes are parallel. The coordinate system of a dimer is shown in Figure 6b, the angle (ϕ) defined by the line perpendicular to the coordinate plane through a metal center and the line connecting Cu···Cu′ being 21.9° for **A**–**A′** and 27.8° for **B**–**B′**. It has been reported that [Cu(salen)][22] forms dimers bridged through O(phenolate) across the crystal-

Table 4. Selected Bond Distances (Å) and Angles (deg) with Their Estimated Standard Deviations in Parentheses for [Cu(HL)] (**1**) and [Cu(HL′)]ClO_4 (**2**)

1			
Bond distances/Å			
Molecule **A**		Molecule **B**	
Cu(1)–O(1)	1.9120(17)	Cu(2)–O(4)	1.914(2)
Cu(1)–O(2)	1.921(2)	Cu(2)–O(5)	1.934(2)
Cu(1)–N(1)	2.003(2)	Cu(2)–N(4)	2.005(2)
Cu(1)–N(2)	1.975(2)	Cu(2)–N(5)	1.974(2)
Bond angles/deg			
O(1)–Cu(1)–O(2)	82.13(9)	O(4)–Cu(2)–O(5)	82.77(8)
O(1)–Cu(1)–N(1)	91.81(9)	O(4)–Cu(2)–N(4)	91.92(8)
O(1)–Cu(1)–N(2)	172.58(10)	O(4)–Cu(2)–N(5)	170.80(6)
O(2)–Cu(1)–N(1)	173.54(8)	O(5)–Cu(2)–N(4)	174.04(10)
O(2)–Cu(1)–N(2)	90.64(9)	O(5)–Cu(2)–N(5)	89.36(9)
N(1)–Cu(1)–N(2)	95.48(9)	N(4)–Cu(2)–N(5)	96.15(9)
2			
Bond distances/Å			
Cu(1)–O(1)	1.9138(17)	Cu(1)–O(2)	1.9313(18)
Cu(1)–N(1)	1.955(2)	Cu(1)–N(2)	1.956(2)
Bond angles/deg			
O(1)–Cu(1)–O(2)	89.26(7)	O(1)–Cu(1)–N(1)	93.16(8)
O(1)–Cu(1)–N(2)	165.06(8)	O(2)–Cu(1)–N(1)	154.01(8)
O(2)–Cu(1)–N(2)	93.01(8)	N(1)–Cu(1)–N(2)	91.26(9)

lographic center of symmetry (Cu···O = 2.414(2) Å), and the complex has a "stepped" configuration, as observed with dimers of [FeCl(salen)][23,24] (Figure 6c-2). Nathan et al.[25] reported the X-ray structures of a series of Cu^{II} complexes with tetradentate Schiff base ligands derived from salicylaldehyde and polymethylenediamines of varying chain lengths. When the number of methylene groups of the alkyl chain is three, the complex ([Cu(saltn)]) has a distorted tetrahedral structure with a dihedral angle of 25.4° between the two Cu–N–O planes and forms a dimeric structure similar to **1** (Figure 6c-1). It is to be noted that **1** is only slightly distorted from planarity, 2.60° for **A** and 5.17° for **B**.

The crystal structures of [Cu(HL)] (**1**) projected along the *a*-axis and the *c*-axis, are shown in Figure S1. Chains composed of molecules **B** run parallel along the *b*-axis, while chains composed of molecules **A** run parallel along the [110] direction. Two kinds of π–π stacking exist in 1D chains; one is within the dimer and the other is between the neighboring dimers. The average π–π stacking distance between the neighboring dimers is 3.19 Å for **A** and 3.28 Å for **B**.

Structural Description of [Cu(HL′)]ClO_4 (2). Compound **2** crystallized in the monoclinic space group $P2_1/c$ (No. 14) with $Z = 4$. The crystal data are summarized in Table 3. A perspective view of the complex with atom numbering scheme is shown in Figure 7. Hydrogen atoms are omitted for clarity. It is evident that one of the arms of the tripodal ligand is detached, probably because of thermal hydrolysis of the imine bond. The amine nitrogen atom thus formed is protonated to form an ammonium ion, the complex being formulated as [Cu(HL′)]ClO_4. The perchlorate ion is not coordinat-

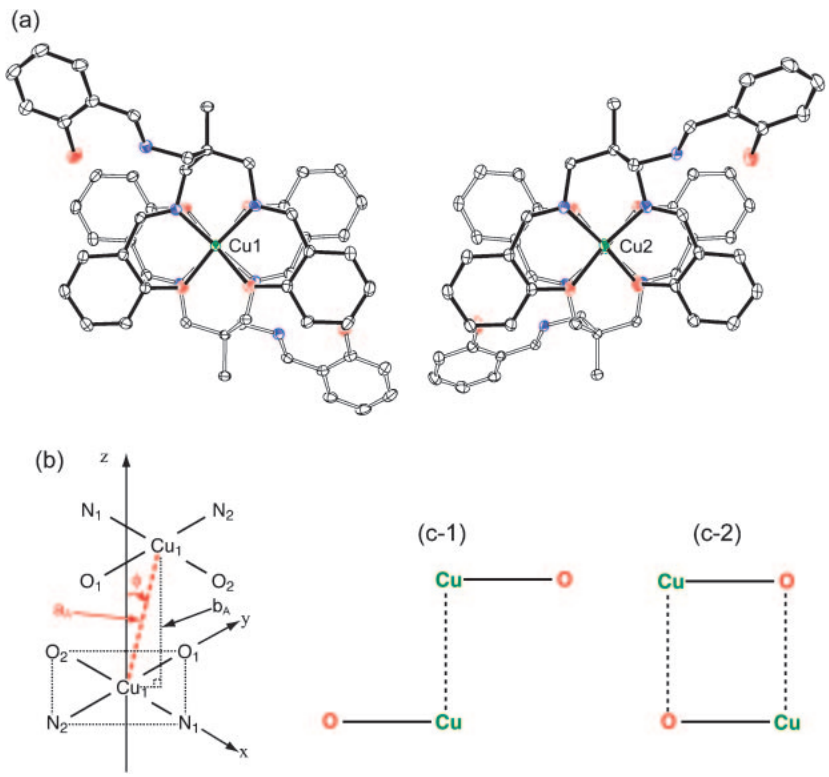

Figure 6. Dimeric structures of [Cu(HL)] (**1**). (a) Structures as viewed along the Cu(1)···Cu(1′) and Cu(2)···Cu(2′) directions. (b) The coordinate system of a dimer. (c) Comparison of the two dimeric structures, [Cu(HL)] (**1**, c-1) and [Cu(salen)] (c-2).

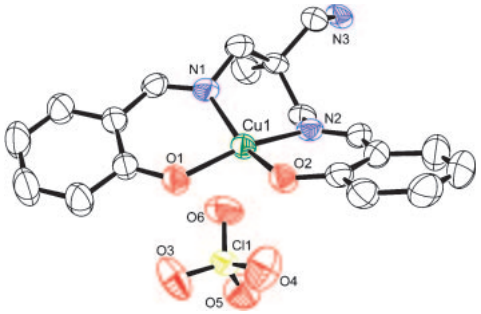

Figure 7. ORTEP view of [Cu(HL′)]ClO_4 (**2**) with atom numbering scheme showing the 50% probability ellipsoids. Hydrogen atoms are omitted for clarity. Color code: green, Cu; blue, N; red, O; black, C; yellow, Cl.

ed, the Cu(1)···O(6) distance being 2.984(2) Å. The coordination arrangement around Cu is distorted square planar; the dihedral angle between the Cu(1)–N(1)–O(1) and Cu(1)–N(2)–O(2) planes is 29.4°.

In the crystal of **2** (Figure S2), adjacent complex cations are connected by N(3)–H(22)···O(1′) and N(3)–H(20)···O(2′) hydrogen bonds with the N(3)···O(1′) and N(3)···O(2′) distances of 2.761(3) and 2.700(3) Å, respectively, to form a one-dimensional chain structure along the *c*-axis. The remaining hydrogen atom, H(21), attached to N(3) is hydrogen bonded to a perchlorate ion (O(4′)) with a N(3)···O(4′) distance of 2.958(3) Å. Furthermore, the neighboring chains are linked by π–π stacking between the chelate moieties of the complex cations with the average distance of 3.39 Å to form a 2D sheet structure on the *bc*-plane.

Structural Description of $[Cu_3(L)_2]\cdot CH_3CN\cdot 2CH_3OH$ (3). The crystal subjected to X-ray crystallography involved an acetonitrile molecule and two methanol molecules as solvent molecules of crystallization. Compound **3** crystallized in the triclinic space group $P\bar{1}$ (No. 2) with $Z = 2$. The crystal data are summarized in Table 3. Compound **3** contains two kinds of molecules, **A** and **B**, in the crystal. Figure 8 shows perspective views of these two molecules with atom numbering schemes. Selected bond distances and angles are listed in Table 5. Molecules **A** and **B** have crystallographic centers of symmetry at Cu(2) and Cu(4), respectively. An imine nitrogen atom and a phenolate oxygen atom of one arm of each terminal unit coordinate to the central Cu^{II} ion to form a trinuclear complex. The central Cu^{II} ions (Cu(2) and Cu(4)) have a perfect square-planar structure with *trans*-N_2O_2 donor atoms, while the terminal Cu^{II} ions (Cu(1) and Cu(3)) have a distorted square-planar structure with *cis*-N_2O_2 donor atoms. The dihedral angle between the Cu(1)–N(1)–O(1) and Cu(1)–N(2)–O(2) planes is 31.38° and that between the Cu(3)–N(4)–O(4) and Cu(3)–N(5)–O(5) planes is 20.65°. The distance between the neighboring Cu ions is 5.9799(6) Å for Cu(1)···Cu(2) and 5.3008(6) Å for Cu(3)···Cu(4).

Figure S3 shows the crystal structure of **3**. The neighboring molecules of the same kind are π–π stacked, and chains composed of molecules **A** and those composed of molecules **B** run parallel along the *b*-axis. The manner of stacking is different between the two chains. The salicylideneamino moieties are stacked in **A**···**A**, while in **B**···**B**, stacking is observed between the ligand moieties including O(phenolate)–C(aromatic)–

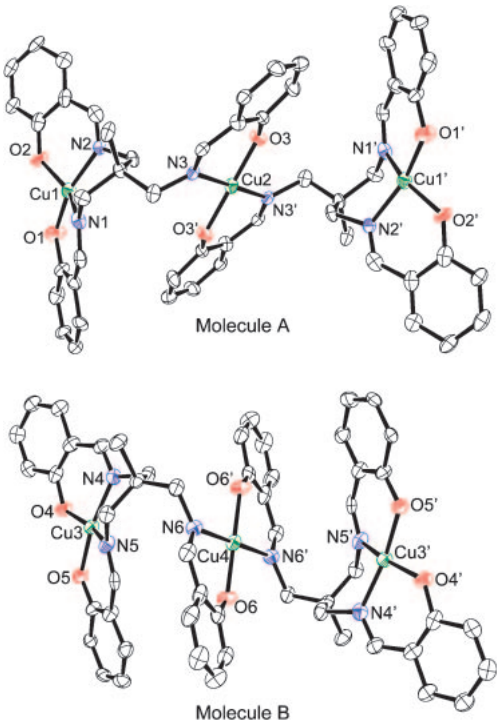

Figure 8. ORTEP views of molecules **A** (top) and **B** (bottom) of $[Cu_3(L)_2]\cdot CH_3CN\cdot 2CH_3OH$ (**3**) with atom numbering scheme showing the 50% probability ellipsoids. The solvent molecules and hydrogen atoms are omitted for clarity. Color code: green, Cu; blue, N; red, O; black, C.

C(aromatic)–C(imine)–N(imine) as in the dimeric structure of [Cu(HL)] (**1**). The average intermolecular π–π stacking distance is 3.30 Å for **A**···**A** (Cu···Cu = 6.9961(8) Å) and 3.80 Å for **B**···**B** (Cu···Cu = 3.9128(9) Å).

Structural Description of $[Cu_3(L)_2]\cdot 2CH_2Cl_2$ (4). The crystal subjected to X-ray crystallography included two dichloromethane molecules. Compound **4** crystallized in the triclinic space group $P\bar{1}$ (No. 2) with $Z = 1$. The crystal data are summarized in Table 3. Figure 9 shows a perspective view of the molecule with atom numbering schemes. Selected bond distances and angles are listed in Table 5. The complex has a crystallographic inversion center at Cu(2). An imine nitrogen atom and a phenolate oxygen atom of one arm of each terminal unit coordinate to the central Cu ion to form a trinuclear complex, as in the case of **3**. The central Cu(2) atom has a perfect square-planar structure with *trans*-N_2O_2 donor atoms, while the terminal Cu(1) and Cu(1′) atoms have a distorted square-planar structure with *cis*-N_2O_2 donor atoms. The dihedral angle between the Cu(1)–N(1)–O(1) and Cu(1)–N(2)–O(2) planes is 34.28°. The distance between Cu(1)···Cu(2) is 4.9830(5) Å and that between Cu(1)···Cu(1′) is 9.9659(7) Å.

Figure S4 shows the crystal structure of **4**. The packing manner is different from that in **3**. Neighboring molecules are π–π stacked between the chelate moieties including O(phenolate)–C(aromatic)–C(aromatic)–C(imine)–N(imine) and a 1D chain structure is formed along the *c*-axis. The average intermolecular π–π stacking distance is 3.88 Å (Cu···Cu = 4.7430(6) Å).

Table 5. Selected Bond Distances (Å) and Angles (deg) with Their Estimated Standard Deviations in Parentheses for $[Cu_3(L)_2]\cdot CH_3CN\cdot 2CH_3OH$ (**3**), and $[Cu_3(L)_2]\cdot 2CH_2Cl_2$ (**4**)

3

Bond distances/Å

Molecule **A**		Molecule **B**	
Cu(1)–N(1)	1.947(4)	Cu(3)–N(4)	1.937(5)
Cu(1)–O(1)	1.876(4)	Cu(3)–N(5)	1.970(3)
Cu(1)–N(2)	1.941(4)	Cu(3)–O(4)	1.896(3)
Cu(1)–O(2)	1.905(3)	Cu(3)–O(5)	1.874(4)
Cu(2)–N(3)	2.004(4)	Cu(4)–O(6)	1.928(4)
Cu(2)–O(3)	1.897(3)	Cu(4)–N(6)	2.030(4)

Bond angles/deg

N(1)–Cu(1)–N(2)	91.52(17)	N(4)–Cu(3)–N(5)	91.30(18)
O(1)–Cu(1)–O(2)	89.84(17)	O(4)–Cu(3)–O(5)	87.45(17)
O(1)–Cu(1)–O(1)	93.00(17)	N(5)–Cu(3)–O(5)	92.51(17)
N(2)–Cu(1)–O(2)	94.43(18)	N(4)–Cu(3)–O(4)	92.51(17)
N(1)–Cu(1)–O(2)	159.18(18)	N(4)–Cu(3)–O(5)	166.45(8)
O(2)–Cu(1)–N(2)	155.42(17)	N(5)–Cu(3)–O(4)	163.67(7)
N(3)–Cu(2)–O(3)	90.74(16)	N(6)–Cu(4)–O(6)	90.99(18)
N(3)–Cu(2)–O(3′)	89.26(16)	N(6)–Cu(4)–O(6′)	89.01(18)
N(3)–Cu(2)–N(3′)	180.0(2)	N(6)–Cu(4)–N(6′)	180.0(2)
O(3)–Cu(2)–O(3′)	180.0(2)	O(6)–Cu(4)–O(6′)	180.0(2)

4

Bond distances/Å

Cu(1)–N(1)	1.962(3)	Cu(1)–O(2)	1.918(3)
Cu(1)–O(1)	1.909(2)	Cu(2)–N(3)	2.005(2)
Cu(1)–N(2)	1.949(3)	Cu(2)–O(3)	1.914(2)

Bond angles/deg

N(1)–Cu(1)–N(2)	95.48(9)	N(2)–Cu(1)–O(1)	172.58(10)
O(1)–Cu(1)–O(2)	82.13(9)	N(3)–Cu(2)–N(3′)	96.15(9)
N(1)–Cu(1)–O(1)	91.81(9)	O(3)–Cu(2)–O(3′)	82.77(8)
N(2)–Cu(1)–O(2)	90.64(9)	N(3)–Cu(2)–O(3)	89.36(9)
N(1)–Cu(1)–O(2)	173.54(8)	N(3)–Cu(2)–O(3′)	91.92(8)

Magnetic Properties of [Cu(HL)] (1) and [Cu(HL′)]ClO_4 (2). Temperature-dependent molar susceptibility measurements of powdered samples of **1** and **2** were carried out at an applied field of 1 T in the temperature range 1.9–300 K. The data are presented as plots of χ_M vs. T and $\chi_M T$ vs. T in Figure 10, where χ_M is the molar magnetic susceptibility and T is the absolute temperature. The $\chi_M T$ value of **1** at 300 K (0.425 $cm^3\,K\,mol^{-1}$) is larger than the spin-only value (0.375 $cm^3\,K\,mol^{-1}$) for a d^9 configuration ($S = 1/2$) but within the range normally found for magnetically diluted copper(II) complexes. The $\chi_M T$ value is almost constant over the entire temperature region except for a steep drop below 12 K. We have seen that the complex consists of dimers formed by π–π stacking of the mononuclear components, and fits to the experimental data were performed using the Bleaney–Bowers equation to take the magnetic interaction within the dimer into consideration. Temperature-independent paramagnetism was also taken into consideration ($N\alpha = 60 \times 10^{-6}$ $cm^3\,mol^{-1}$). The best-fit parameters obtained are $g(Cu) = 2.05$ and $J = -0.46\,cm^{-1}$. Compound **1** contains two independent but similar molecules, **A** and **B**, in the crystal, and the magnetic data should be the average for these molecules. The negative

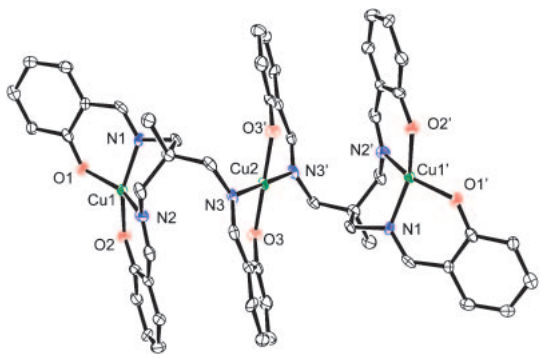

Figure 9. ORTEP view of molecules of $[Cu_3(L)_2]\cdot 2CH_2Cl_2$ (**4**) with atom numbering scheme showing the 50% probability ellipsoids. The solvent molecules and hydrogen atoms are omitted for clarity. Color code: green, Cu; blue, N; red, O; black, C.

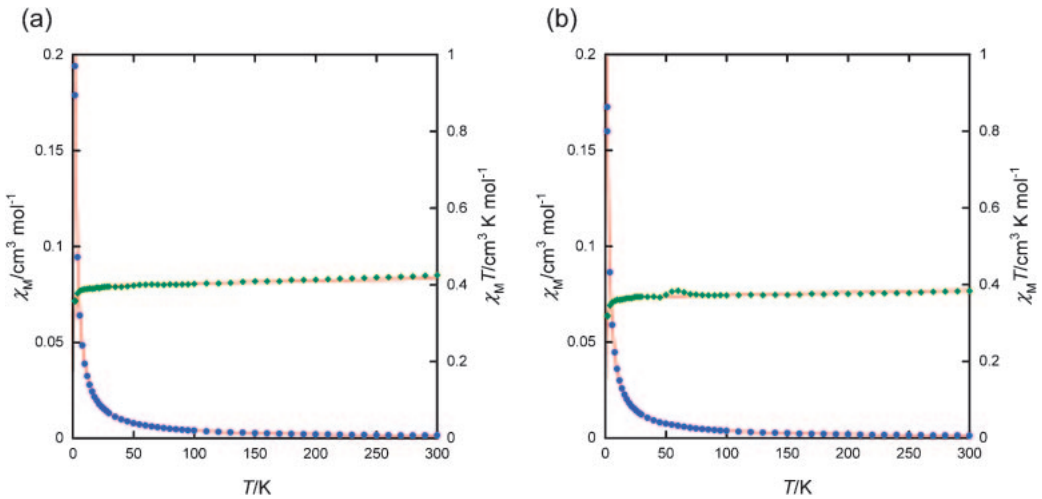

Figure 10. Magnetic behaviors of (a) [Cu(HL)] (**1**) and (b) [Cu(HL′)]ClO_4 (**2**) in the form of χ_M vs. T and $\chi_M T$ vs. T plots. The solid lines are generated from the best-fit magnetic parameters (cf. text).

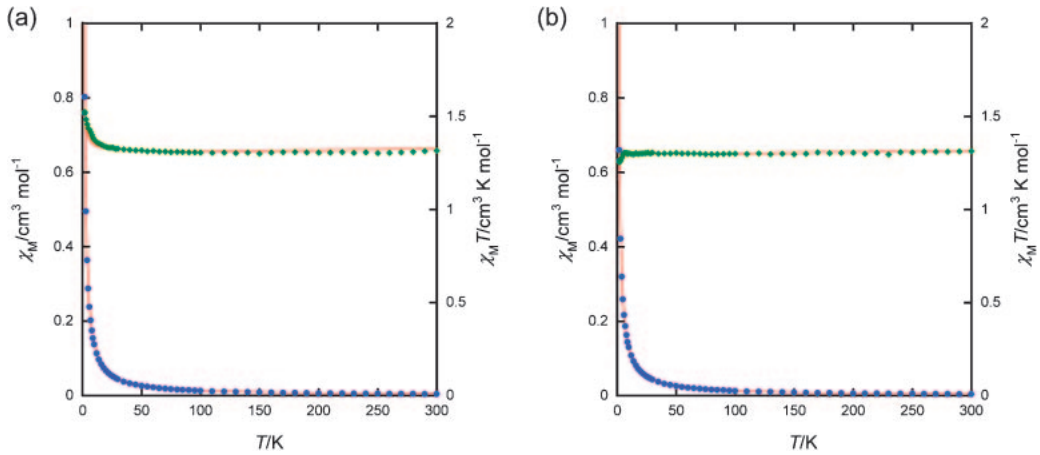

Figure 11. Magnetic behaviors of (a) $[Cu_3(L)_2]\cdot CH_3CN\cdot 2CH_3OH$ (**3**) and (b) $[Cu_3(L)_2]\cdot 2CH_2Cl_2$ (**4**) in the form of χ_M vs. T and $\chi_M T$ vs. T plots. The solid lines are generated from the best-fit magnetic parameters (cf. text).

J value indicates that antiferromagnetic interaction operates in **1**. We ignored the interdimer interaction, because the magnetic interaction between the dimers should be negligibly small (see Figure S1). The J value is small as we expected from the structural data. It should be noted that the corresponding intradimer exchange parameter for [Cu(salen)] is ferromagnetic ($J = +9.3\,cm^{-1}$),[26] where the dimeric structure is different from that of **1**.

The $\chi_M T$ value of **2** at 300 K (0.383 cm^3 K mol^{-1}) is nearly the same as for the spin-only value (0.375 cm^3 K mol^{-1}) for a d^9 configuration ($S = 1/2$). The $\chi_M T$ value is almost constant except for a steep drop below 16 K. We notice that **2** also involves π–π stacking between the chelate moieties of the mononuclear units as **1** does. By using the same method as for **1**, we obtained the following parameters. g(Cu) = 1.98, $J = -0.64\,cm^{-1}$ for **2**.

Magnetic Properties of $[Cu_3(L)_2]\cdot CH_3CN\cdot 2CH_3OH$ (3) and $[Cu_3(L)_2]\cdot 2CH_2Cl_2$ (4). The magnetic susceptibility measurements for **3** and **4** were carried out under the same conditions as for **1** and **2**, the data being presented as plots of χ_M vs. T and $\chi_M T$ vs. T in Figure 11. The $\chi_M T$ value of **3** at 300 K (1.317 cm^3 K mol^{-1}) is larger than the spin-only value (1.125 cm^3 K mol^{-1}) for three independent d^9 configurations ($S = 1/2$) but within the range normally found for such complexes. The $\chi_M T$ value is almost constant over the entire temperature region, except for a steep increase below 10 K. A relatively large number of triangular or linear Cu1Cu2-Cu1-type trinuclear species have been described.[27] There are two equal Cu1–Cu2 and Cu1′–Cu2 interaction pathways and a Cu1–Cu1′ pathway in **3**. Because the Cu(1)···Cu(2) distance (av. 5.6404(6) Å) and the Cu(1)···Cu(1′) distance (av. 11.2806(9) Å) are large, and the bridging group involves magnetically noninteracting sp^3 carbon atoms, we assumed the intramolecular magnetic interaction $J_{Cu1\text{–}Cu2} = J_{Cu1'\text{–}Cu2} = 0$ and $J_{Cu1\text{–}Cu1'} = 0$. Thus, fits to the experimental data were performed using eq 1 which is the sum of the susceptibility for three magnetically independent Cu^{II}. N, β, and k are the Avogadro constant, electronic Bohr magneton, and Boltzmann constant, respectively. Two g factors g_{Cu1} and g_{Cu2} are employed because the geometries are difference between Cu(1) and Cu(2). Temperature-independent paramagnetism was also taken into consideration ($N\alpha = 60 \times 10^{-6}\,cm^3\,mol^{-1}$). Weiss constant θ was introduced to evaluate the intermolecular magnetic interaction.

$$\chi_M = \frac{N\beta^2}{4k(T-\theta)}(2g_{Cu1}{}^2 + g_{Cu2}{}^2) + N\alpha. \quad (1)$$

Compound **3** contains two independent but similar molecules, **A** and **B**, in the crystal, and the parameters obtained should be the average for these molecules. The best-fit parameters obtained are as follows; $g_{Cu1} = g_{Cu1'} = 2.23$, $g_{Cu2} = 2.16$, and $\theta = 0.19\,cm^{-1}$. The intermolecular coupling constant J was calculated using eq 2. The crystal structure analysis of **3** showed that each molecule is linked with two neighboring molecules through π–π interaction, and thus $z = 2$. The calculation ($z = 2$, $S = 1/2$) gives $J = +0.13\,cm^{-1}$.

$$\theta = [2zJS(S+1)]/3k. \quad (2)$$

The $\chi_M T$ value of **4** at 300 K (1.314 cm^3 K mol^{-1}) is almost the same as for **3** at 300 K (1.317 cm^3 K mol^{-1}), this value being larger than the spin-only value (1.125 cm^3 K mol^{-1}) for three independent d^9 configurations ($S = 1/2$). The $\chi_M T$ value is almost constant over the entire temperature region except for a slight decrease below 5 K. The data were analyzed by the same procedure as for **3** to give the best-fit parameters: $g_{Cu1} = g_{Cu1'} = 2.19$, $g_{Cu2} = 2.09$, and $\theta = -0.08\,cm^{-1}$. The negative θ value indicates that there exists antiferromagnetic interaction between the molecules. By using eq 2, we obtained the intermolecular coupling constant $J = -0.06\,cm^{-1}$. The J value is negative as opposed to the positive value for **3**. The extremely weak antiferromagnetic interaction ($J = -0.06\,cm^{-1}$) in **4** between the trinuclear molecules can be explained in terms of the weak π–π stacking. In the crystal of **4**, neighboring molecules are π–π stacked between the chelate moieties as in **1** and **2**, both of which exhibit an antiferromagnetic interaction ($-0.46\,cm^{-1}$ in **1**; $-0.64\,cm^{-1}$ in **2**). The average intermolecular π–π stacking distance for **4** (3.88 Å) is larger than those for **1** (3.33 and 3.18 Å) and **2** (3.39 Å) to weaken the antiferromagnetic interaction. Complex **3** exhibit a small ferromagnetic interaction ($J = +0.13\,cm^{-1}$), and we can explain it as the result of two competing interactions. In the crystal of **3**, there are two kinds of intermolecular π–π stacking in-

teractions, i.e., the stacking between the chelate moieties and the stacking between the salicylideneamino moieties. All the other complexes, **1**, **2**, and **4**, involve only stacking between the chelate moieties and they exhibit an antiferromagnetic interaction. We presume that the stacking between the chelate moieties and the stacking between the salicylaldehyde moieties induces an antiferromagnetic and a ferromagnetic interaction, respectively. Although both the antiferromagnetic and ferromagnetic interactions operate in **3**, the ferromagnetic interaction seems to surpass the antiferromagnetic interaction because the latter is negligibly small due to a large π–π stacking distance (3.80 Å). Thus, a small ferromagnetic interaction is observed in **3**.

Concluding Remarks

By the reaction of H_3L and Cu^{II}, we obtained four kinds of Cu complexes. Two of them are mononuclear, [Cu(HL)] (**1**) and [Cu(HL′)]ClO_4 (**2**), and the others are trinuclear, $[Cu_3(L)_2]\cdot CH_3CN\cdot 2CH_3OH$ (**3**) and $[Cu_3(L)_2]\cdot 2CH_2Cl_2$ (**4**). In **2**, one of the three arms was disconnected probably because of hydrolysis. Although the chemical formulas of the Cu^{II} complexes are the same as those of the Ni^{II} complexes, $[M^{II}(HL)]$ and $[M^{II}{}_3(L)_2]$ (M = Cu and Ni), the coordination arrangement around the metal ion is different; square planar (Cu^{II}) vs. octahedral (Ni^{II}). The electronic spectra and electrochemical properties of **1** and **2** are quite similar to each other, because they have similar molecular structures. The two trinuclear complexes, **3** and **4**, also have a similar molecular structure to each other, and their solution properties are identical. All of the complexes, **1**–**4**, involve π–π stacking interactions between the molecules in the crystal structures, which are responsible for weak magnetic interactions. Of all the complexes, only **3** shows a ferromagnetic interaction. The difference in magnetic interactions, ferromagnetic and antiferromagnetic, seems to be due to the different π–π stacking modes between the molecules. In the crystal structure of **3**, there are two kinds of intermolecular π–π stacking interactions, i.e., the stacking between the chelate moieties and the stacking between the salicylideneamino moieties. All the other complexes, **1**, **2**, and **4**, involve only stacking between the chelate moieties. Thus, we presume that the stacking between the chelate moieties and the stacking between the salicylaldehyde moieties induces an antiferromagnetic and a ferromagnetic interaction, respectively. Although both antiferromagnetic and ferromagnetic interactions exist in **3**, the ferromagnetic interaction seems to be a little larger than the antiferromagnetic interaction resulting in the overall ferromagnetic interaction. The extremely small antiferromagnetic interaction observed in **4** can be explained in terms of the weak π–π stacking.

Experimental

Caution. Perchlorate salts of metal complexes are potentially explosive. Only small quantities of material should be prepared and the samples should be handled with care.

Materials. All reagents and solvents in the syntheses were of reagent grade, and they were used without further purification. Tris(aminomethyl)ethane was prepared by the method of Fleischer et al.,[28] and the Schiff base ligand, H_3L, was prepared by a method reported previously.[9]

[Cu(HL)]·0.5H_2O (1). An ethanol solution (5 cm^3) of $Cu(CH_3COO)_2\cdot H_2O$ (20 mg, 0.10 mmol) was added to a suspension of H_3L (128 mg, 0.30 mmol) in ethanol (10 cm^3), and the mixture was stirred at room temperature. After the reaction mixture was filtered, the filtrate was allowed to stand for several days to give green crystals. Yield 48 mg (49%). Recrystallization from dichloromethane–ethanol afforded crystals of diffraction quality. Anal. Found: C, 62.78; H, 5.15; N, 8.42%. Calcd for $C_{26}H_{26}CuN_3O_{3.5}$ = [Cu(HL)]·0.5H_2O (**1**): C, 62.45; H, 5.24; N, 8.40%. IR (KBr disk): ν(C=N_{imine}) 1622, 1640 (sh) cm^{-1}.

[Cu(HL′)]$ClO_4\cdot H_2O$ (2). Triethylamine (10 mg, 0.10 mmol) was added to a suspension of H_3L (85 mg, 0.20 mmol) in ethanol (10 cm^3), and the mixture was heated to give a pale yellow solution. $Cu(ClO_4)_2\cdot 6H_2O$ (37 mg, 0.10 mmol) in ethanol (5 cm^3) was added to this solution, and the mixture was stirred for 10 h at room temperature. The resulting green precipitate was collected by filtration. Yield: 24 mg (47%). The product was recrystallized from acetonitrile–ethanol. Anal. Found: C, 45.33; H, 4.28; N, 7.79%. Calcd for $C_{19}H_{24}ClCuN_3O_7$ = [Cu(HL′)]$ClO_4\cdot H_2O$ (**2**): C, 45.15; H, 4.79; N, 8.31%. IR (KBr disk): ν(N–H) 3131; ν(C=N_{imine}) 1626; ν(ClO_4^-) 1157, 1110, 1088 cm^{-1}.

[$Cu_3(L)_2$]·$CH_3CN\cdot 2CH_3OH$ (3). A methanol solution (15 cm^3) of $Cu(CH_3COO)_2\cdot H_2O$ (30 mg, 0.15 mmol) and a methanol solution (5 cm^3) of triethylamine (30 mg, 0.30 mmol) were added to an acetonitrile solution (25 cm^3) of H_3L (43 mg, 0.10 mmol), and the mixture was stirred vigorously. After the reaction mixture was filtered, the filtrate was allowed to stand for a few days to give green crystals. They were collected by filtration. Yield 45 mg (40%). Anal. Found: C, 57.12; H, 4.66; N, 7.75%. Calcd for $C_{53}H_{56}Cu_3N_6O_9$ = [$Cu_3(L)_2$]·$CH_3OH\cdot 2H_2O$: C, 57.26; H, 5.08; N, 7.56%. The crystals ([$Cu_3(L)_2$]·$CH_3CN\cdot 2CH_3OH$ (**3**)) obtained by recrystallization from CH_3CN–CH_3OH were used for X-ray structure analysis and other measurements. IR (KBr disc): ν(C=N_{imine}) 1626 cm^{-1}.

[$Cu_3(L)_2$]·$2CH_2Cl_2$ (4). An ethanol solution (15 cm^3) of $Cu(CH_3COO)_2\cdot H_2O$ (30 mg, 0.15 mmol) and an ethanol solution (5 cm^3) of triethylamine (30 mg, 0.30 mmol) were added to a dichloromethane solution (25 cm^3) of H_3L (43 mg, 0.10 mmol), and the mixture was stirred vigorously. After the reaction mixture was filtered, the filtrate was allowed to stand for a few days to give green crystals. They were collected by filtration. Yield 67 mg (55%). Anal. Found: C, 53.12; H, 4.20; N, 6.86%. Calcd for $C_{54}H_{52}Cl_4Cu_3N_6O_6$ = [$Cu_3(L)_2$]·$2CH_2Cl_2$ (**4**): C, 53.45; H, 4.32; N, 6.93%. IR (KBr disk): ν(C=N_{imine}) 1623 cm^{-1}.

Physical Measurements. UV–visible absorption spectra were recorded using a JASCO Ubest-550 spectrophotometer, and the infrared spectra were measured using a JASCO FT/IR-550 spectrophotometer. The magnetic susceptibilities were measured using a Quantum Design MPMS SQUID magnetometer in the temperature range 1.9–300 K at an applied magnetic field of 1 T. A diamagnetic correction was applied using Pascal's constants.[27] Elemental analyses were carried out on a Perkin-Elmer 2400II elemental analyzer. Cyclic voltammetry measurements were performed using a Fuso HECS 321B potential sweep unit and a Fuso HECS 312B potentiostat with dimethyl sulfoxide (DMSO) solutions containing Bu_4NBF_4 (0.1 M) as the supporting electrolyte. The electrochemical cell was a three-electrode system consisting of a glassy carbon working electrode, a platinum wire auxiliary electrode, and an Ag/Ag^+ ($Ag/0.01$ M $AgNO_3$) reference electrode. As an external standard, the Fc/Fc^+ (Fc = ferrocene) couple was observed at +0.17 V vs. Ag/Ag^+ under the same conditions. Coulometric studies were carried out on the same appara-

tus using a platinum gauze as a working electrode.

X-ray Data Collection, Reduction, and Crystal Structure Determination. Each single crystal of **1**–**3** was sealed in a glass capillary with the mother liquor to prevent loss of the solvent molecules of crystallization. A crystal of **4** was mounted by using the MicroMesh™ method. The X-ray measurements were made on a Rigaku RAXIS RAPID II imaging plate area detector with graphite monochromated Mo Kα radiation ($\lambda = 0.71069$ Å). The structures were solved using direct methods (SIR2004,[29] SIR92,[30] SHELX97[31]), and expanded using Fourier techniques. The structures were refined by full-matrix least-squares based on F^2. All calculations were performed using the CrystalStructure crystallographic software package.[32] Crystallographic data have been deposited with Cambridge Crystallographic Data Centre: Deposition numbers CCDC-677299, -677300, -677301, and -677302 for **1**, **2**, **3**, and **4**, respectively. Copies of the data can be obtained free of charge via http://www.ccdc.cam.ac.uk/conts/retrieving.html (or from the Cambridge Crystallographic Data Centre, 12, Union Road, Cambridge, CB2 1EZ, UK; Fax: +44 1223 336033; e-mail: deposit@ccdc.cam.ac.uk).

This work was supported in part by a Grant-in-Aid for Scientific Research (No. 17350028) from the Ministry of Education, Culture, Sports, Science and Technology of Japan, and by the Iketani Science and Technology Foundation. T. Y. was supported by the JSPS program for Research Fellowships for Young Scientists (No. 17003601).

Supporting Information

Crystal structures of [Cu(HL)] (**1**) (Figure S1), [Cu(HL′)]ClO_4 (**2**) (Figure S2), $[Cu_3(L)_2]\cdot CH_3CN\cdot 2CH_3OH$ (**3**) (Figure S3), and $[Cu_3(L)_2]\cdot 2CH_2Cl_2$ (**4**) (Figure S4). This material is available free of charge on the Web at: http://www.csj.jp/journals/bcsj/.

References

1 F. P. Dwyer, N. S. Gill, E. C. Gyarfas, F. Lions, *J. Am. Chem. Soc.* **1957**, *79*, 1269.

2 Y. Urushigawa, M. Yuki, H. Ishikita, T. Inazu, T. Yoshino, *Mem. Fac. Sci., Kyushu Univ., Ser. C* **1977**, *10*, 125.

3 M. A. Green, M. J. Welch, J. C. Huffman, *J. Am. Chem. Soc.* **1984**, *106*, 3689.

4 D. F. Evans, D. A. Jakubovic, *J. Chem. Soc., Dalton Trans.* **1988**, 2927.

5 S. Liu, E. Wong, V. Karumaratne, S. J. Rettig, C. Orvig, *Inorg. Chem.* **1993**, *32*, 1756.

6 M. G. B. Drew, C. J. Harding, V. McKee, G. G. Morgan, J. Nelson, *J. Chem. Soc., Chem. Commun.* **1995**, 1035.

7 M. E. Marmion, S. R. Woulfe, W. L. Newmann, G. Pilcher, D. N. Nosco, *Nucl. Med. Biol.* **1996**, *23*, 567.

8 M. Kojima, S. Azuma, M. Hirotsu, K. Nakajima, M. Nonoyama, Y. Yoshikawa, *Chem. Lett.* **2000**, 482.

9 H. Ohta, K. Harada, K. Irie, S. Kashino, T. Kambe, G. Sakane, T. Shibahara, S. Takamizawa, W. Mori, M. Nonoyama, M. Hirotsu, M. Kojima, *Chem. Lett.* **2001**, 842.

10 M. Kojima, H. Ohta, *Challenges Coord. Chem. New Century* **2001**, *5*, 65.

11 M. Kojima, *Mol. Cryst. Liq. Cryst.* **2000**, *342*, 39.

12 T. Kobayashi, T. Yamaguchi, Y. Sunatsuki, M. Kojima, H. Akashi, N. Re, N. Matumoto, 56th Symposium on Coordination Chemistry of Japan, Hiroshima, September, **2006**, Abstr., No. 2Ac05, to be published; manuscript in preparation.

13 T. Kobayashi, T. Yamaguchi, H. Ohta, Y. Sunatsuki, M. Kojima, N. Re, M. Nonoyama, N. Matsumoto, *Chem. Commun.* **2006**, 1950.

14 T. Yamaguchi, Y. Sunatsuki, M. Kojima, H. Akashi, M. Tsuchimoto, N. Re, S. Osa, N. Matsumoto, *Chem. Commun.* **2004**, 1048.

15 K. Nakamoto, *Infrared and Raman Spectra of Inorganic and Coordination Compounds, Part B*, 5th ed., John Wiley & Sons, New York, **1997**.

16 R. S. Downing, F. L. Urbach, *J. Am. Chem. Soc.* **1969**, *91*, 5977.

17 R. L. Belford, T. S. Piper, *Mol. Phys.* **1962**, *5*, 251.

18 R. L. Belford, W. A. Yeranos, *Mol. Phys.* **1963**, *6*, 121.

19 G. V. Panova, V. M. Potapov, I. M. Turovets, E. G. Golub, *Zh. Obshch. Khim.* **1983**, *53*, 1612.

20 S. I. Perry, R. S. Quinn, E. P. Dudek, *Inorg. Chem.* **1968**, *7*, 814.

21 B. Bosnich, *J. Am. Chem. Soc.* **1968**, *90*, 627.

22 M. M. Bhadbhade, D. Srinivas, *Inorg. Chem.* **1993**, *32*, 6122.

23 M. M. Gerloch, J. Lewis, F. E. Mabbs, A. Richards, *Nature* **1966**, *212*, 809.

24 M. M. Gerloch, F. E. Mabbs, *J. Chem. Soc. A* **1967**, 1900.

25 L. C. Nathan, J. E. Koehne, J. M. Gilmore, K. A. Hannibal, W. E. Dewhirst, T. D. Mai, *Polyhedron* **2003**, *22*, 887.

26 a) W. E. Hatfield, *Inorg. Chem.* **1972**, *11*, 216. b) G. O. Carlisle, G. D. Simpson, W. E. Hatfield, *Inorg. Nucl. Chem. Lett.* **1973**, 1247.

27 O. Kahn, *Molecular Magnetism*, VCH, Weinheim, **1993**, Chap. 10.

28 E. B. Fleischer, A. E. Gebala, A. Levey, P. A. Tasker, *J. Org. Chem.* **1971**, *36*, 3042.

29 SIR2004: M. C. Burla, R. Caliandro, M. Camalli, B. Carrozzini, G. L. Cascarano, L. De Caro, C. Giacovazzo, G. Polidori, R. Spagna, *J. Appl. Crystallogr.* **2005**, *38*, 381.

30 A. Altomare, G. Cascarano, C. Giacovazzo, A. Guagliardi, M. C. Burla, G. Polidori, M. Camalli, *J. Appl. Crystallogr.* **1994**, *27*, 435.

31 G. M. Sheldrick, *SHELX 97*, University of Göttingen, Germany, **1997**.

32 *CrystalStructure 3.8, Crystal Structure Analysis Package*, Rigaku and Rigaku/MSC, The Woodlands, TX, USA, **2001–2006**.